Intrinsic magnetic properties of SmFe12–xVx alloys with reduced V-concentration

A.M. Schönhöbel, Rajasekhar Madugundo, O. Yu. Vekilova, O. Eriksson, H.C. Herper, J.M. Barandiarán, G.C. Hadjipanayis

Intrinsic Magnetic Properties of $SmFe_{12-x}V_x$ Alloys with reduced V-concentration

A. M. Schönhöbel[a,b,*], R. Madugundo[a], O. Yu. Vekilova[c], O. Eriksson[c,d], H. C. Herper[c], J. M. Barandiarán[b,a], G. C. Hadjipanayis[e]

[a] *BCMaterials, UPV/EHU Science Park, 48940 Leioa, Spain*
[b] *Department of Electricity and Electronics, University Basque Country (UPV/EHU), 48940 Leioa, Spain*
[c] *Department of Physics and Astronomy, Uppsala University, Box 516, 75121 Uppsala, Sweden*
[d] *School of Science and Technology, Örebro University, SE-70182 Örebro, Sweden*
[e] *Department of Physics and Astronomy, University of Delaware, Newark, DE, 19716, USA*

Abstract

In this work, we present experimental and theoretical results on $SmFe_{12-x}V_x$ (x = 0.5-2.0) alloys with the $ThMn_{12}$ (1:12) structure as possible candidates for rare earth-lean permanent magnets. The compound with $x = 2$ has been previously reported to have a Curie temperature of 330°C, saturation magnetization of about 80 Am^2/kg, and anisotropy field around 9 T. We have synthesized the $SmFe_{11}V$ compound with a nearly pure 1:12 phase; the $x = 0.5$ compound couldn't be synthesized. The stability of the $x = 1$ compound was also confirmed theoretically by calculations of their formation enthalpies using first principles. The newly synthesized $SmFe_{11}V$ compound has a Curie temperature of 361°C and saturation magnetization of 115 Am^2/kg (1.12 T). The anisotropy field has been obtained in magnetically-oriented fine powders, and is around 11 T. These parameters make $SmFe_{11}V$ a good candidate for a new kind of high energy, rare earth-lean permanent magnets.

Keywords: rare-earth lean permanent magnets, $ThMn_{12}$-type structure, iron alloys, magnetocrystalline anisotropy, ab initio calculations, density functional theory

1. Introduction

After the discovery of $R_2Fe_{14}B$ (R=rare-earth) compounds with excellent magnetic properties, research and development in the field of permanent magnets has been focused almost exclusively on these alloys. However, in the last decade, because of the exponentially increasing demand for these magnets, increasing cost and supply risks involving the R-metals, there has been a renewed interest in the $ThMn_{12}$-type (1:12) compounds [1, 2, 3, 4]. These compounds contain only a 7.7% of R, compared with 11.8% in $R_2Fe_{14}B$, and they have a non-cubic structure (tetragonal), which is a requirement for uniaxial magnetocrystalline anisotropy (c-axis for R=Sm and easy plane for R=Nd). The RFe_{12} binary compounds do not exist in the bulk alloy form, but can be stabilized by adding a third element such as Ti, V, Mo, Cr, W or Si [5, 6, 7]. However, addition of this element decreases the saturation magnetization (M_s) and Curie temperature (T_C) [5, 8, 9]; because of this, it is important to keep their concentration as low as possible. So far the 1:12 structure for the $SmFe_{12-x}V_x$ alloys has been obtained for high V concentration ($x \leq 1.5$) and it is very difficult to synthesize as a single-phase material[10, 11, 12]. In order to obtain high coercivity (H_c), it is necessary to avoid the formation of the soft-magnetic α-Fe phase. One of the challenges for the processing of these alloys, therefore, is to obtain a single-phase 1:12 alloy with the minimum V concentration. Previous results have reported the stabilization of 1:12 in this system for $x = 2$ for samples annealed at 850-1050°C for 1-14 days and for $x = 1.5$ annealed at 900-1000°C for 7 days. Sugimoto et al. [13] obtained a phase relation in Sm-Fe-V alloys and reported that the 1:12 phase was only stable for $x > 1.4$. In this work, we studied experimentally and theoretically these compounds to extend the stability range in an effort to increase the magnetization and anisotropy.

Theoretical calculations of magnetocrystalline anisotropy (MAE) of R-based compounds are challenging due to involved small numbers and therefore require very accurate numerical methods. Calculations from first principles, within the VASP simulation package and full-potential LMTO method, were performed to study the electronic structure, the thermodynamic stability, and magnetic properties of these compounds.

2. Methods

2.1. *Experimental*

Ingots of $SmFe_{12-x}V_x$ alloys were prepared by arc-melting the pure metals in Ar atmosphere. The ingots were re-melted four times to insure homogeneity. Samarium loss during the melting was compensated by adding an appropriate excess amount and weighing the alloy after each melting. After arc-melting, the ingots were sealed in quartz tubes filled with Ar and homogenized at temperatures in the range of 900-1100°C for 1-3 days and then quenched in water. X-ray diffraction (XRD) analysis was performed on randomly oriented powders by using a Rigaku Ultima IV diffractometer with Cu-K_α radiation in the Bragg-Brentano geometry. The annealed ingots were

*Corresponding author
Email address: ana.schonhobel@bcmaterials.net (A. M. Schönhöbel)

ground in a mortar and the fine powders were subsequently mixed with an epoxy and aligned in a magnetic field of 2 T. Magnetization curves were measured parallel and perpendicular to the alignment direction by using a vibrating sample magnetometer with a superconducting magnet by applying a maximum field of 12 T. Besides the magnetic measurements, x-ray diffraction on aligned samples was performed to detect the easy magnetization direction. The T_C was determined by using thermogravimetric analysis (TGA). In this measurement, the sample was placed inside an empty, tared TGA pan located near a magnet. Microstructure studies were carried out with a JEOL 100C scanning electron microscope (SEM) equipped with a backscattered electron detector and an energy dispersive x-ray detector system (EDS). The Mössbauer spectra were obtained at room temperature on a conventional constant-acceleration spectrometer with a ^{57}Co source in Rh matrix. The resulting spectra have been fitted with Normos and the errors were at most 0.2 T for the hyperfine fields and 0.01 mm/s for the isomer shifts. The observed linewidths in the magnetic spectra were 0.36 mm/s. The area ratio of the absorption lines was assumed to be 3:2:1:1:2:3 as the absorber was formed by randomly oriented particles.

2.2. *Theoretical*

The $Sm(FeV)_{12}$ phase was studied from first principles. For the electronic structure, lattice parameters and phase stability, the Vienna Ab Initio Simulation Package (VASP) [14, 15, 16] was used within the projector augmented wave (PAW) method [17]. The electronic exchange and correlation effects were treated by the generalized gradient approximation (GGA) in the Perdew, Burke, and Ernzerhof (PBE) form [18]. A 13 atom cell of $SmFe_{12-x}V_x$, where $x = 1$ and 2, was considered. The plane-wave energy cut-off was set to 268 eV. The converged k-point mesh was found to be 16×16×16 Monkhorst-Pack k-points [19]. For the estimation of phase stability of ternary compounds the following equation was used:

$$\Delta H_f = \frac{1}{26}\begin{bmatrix} 2H\,(SmFe_{12-x}V_x) - H\,(Sm_2Fe_{17}) \\ -2xH\,(V) - (7-2x)\,H\,(\alpha\text{-Fe}) \end{bmatrix} \qquad (1)$$

where $x = 1, 2$ is the number of V atoms in the cell on the Fe sublattice. The enthalpy of the $SmFe_{12-x}V_x$ system was calculated and compared with the enthalpy of another phase stable at these conditions (Sm_2Fe_{17}) as well as with the enthalpy of pure elements, V and α-Fe. The obtained VASP lattice parameters were used for the calculation of the magnetic properties with help of the highly accurate all-electron full-potential linear muffin-tin orbital (FP-LMTO) method implemented in the RSPt code [20, 21]. We performed integration over the Brillouin zone, using the tetrahedron method with Blochl's correction [22]. The k-point convergence of the MAE for the chosen supercell size was found when increasing the Monkhorst-Pack mesh [19] to 24×24×24 and it was further used in all calculations. For the treatment of the $4f$ electrons of rare-earth Sm atom the spin polarized core approximation was used.

3. Results and Discussion

3.1. *Experimental*

The XRD patterns of $SmFe_{12-x}V_x$ alloys with different V concentration heat-treated at 1000°C for 2 days are presented in Fig. 1. Apart from the sample with $x = 0.5$, the main phase in all the samples is $ThMn_{12}$-type (space group $I4/mmm$), with a very low α-(Fe,V) around 0.5-1%.

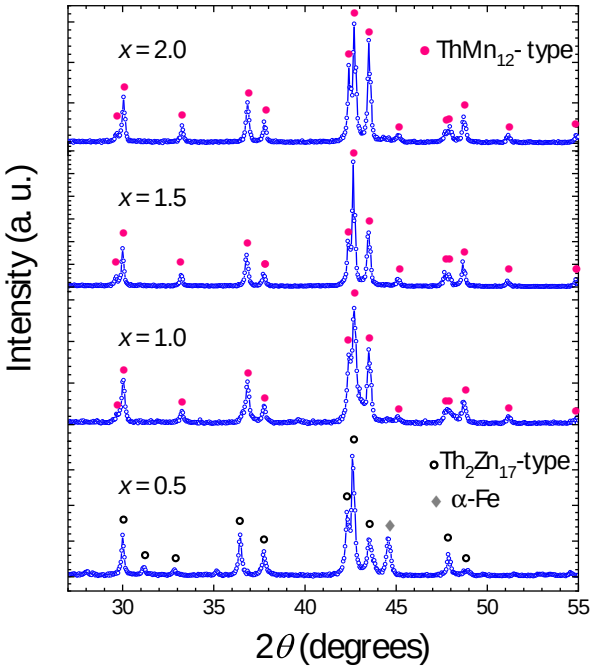

Figure 1: XRD patterns of $SmFe_{12-x}V_x$ alloys with different V concentration annealed at 1000°C.

For the series, the parameters a and c decrease almost linearly from 8.5302 Å^3 and 4.7693 Å^3 to 8.5205 Å^3 and 4.7686 Å^3, respectively with decreasing V concentration as it can be seen in Fig 2(a). The lattice contraction with decreasing V concentration makes the characteristic 1:12 peaks to shift slightly towards higher angles. This is reasonable considering the atomic radius of V (205 pm), which is larger than that of Fe (126 pm), and this also is in agreement with the decreasing of the 1:12 cell volume from 347.04 Å^3 to 346.22 Å^3. At $x = 0.5$, the rhombohedral Th_2Zn_{17}-type structure and α-(Fe,V) were observed, for this concentration we performed different heat treatments in the range of 900°C-1100°C for 1 and 3 days but it was not possible to stabilize the 1:12 phase.

SEM backscattered images of as cast and annealed $SmFe_{11}V$ samples are shown in Fig. 3. Examination of the as cast sample (Fig. 3(a) and 3(b)) revealed the existence of $Sm(Fe,V)_2$, $Sm(Fe,V)_{12}$ and α-(Fe,V) phases. The $Sm(Fe,V)_2$ corresponds to the light grey areas, the 1:12 corresponds to the dark grey areas and α-(Fe,V) to the darker inclusions. The excess Sm appears as lighter inclusions, which are more visible in Fig. 3(b). After annealing, no phase contrast was observed in the SEM back scattered image (Fig. 3(c)), confirming the nearly pure $SmFe_{11}V$ phase.

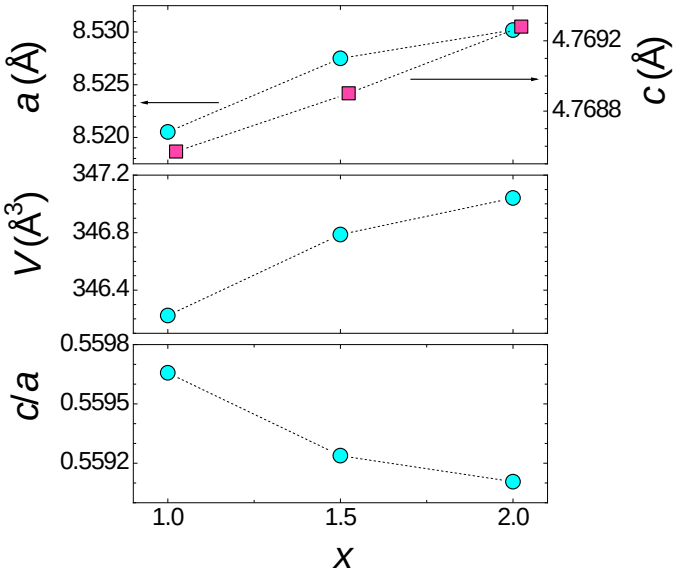

Figure 2: Variation in the structural parameters with different V concentration x. (a) lattice parameters a and c (b) cell volume V and (c) ratio c/a

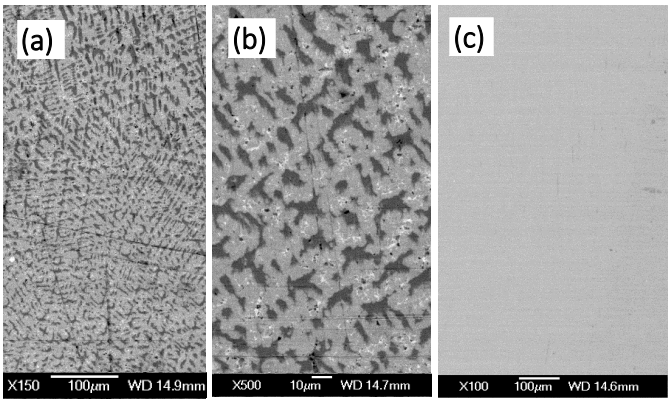

Figure 3: SEM backscattered images of $SmFe_{11}V$ (a) as cast sample at low magnification (b) as cast sample at high magnification and (c) annealed sample.

The T_C were determined by using a thermogravimetric analyser with a magnet. An example plot, for $x = 1$, is shown in the inset of the Fig. 4. When heated, the sample loses its ferromagnetic properties at T_C, resulting in a mass gain that can be detected by the TGA. As Fig. 4 displays, the T_C increases when V concentration is reduced. The T_C of $SmFe_{12-x}V_x$ compounds is determined by the Sm-Sm, Sm-V, Sm-Fe and Fe-Fe exchange interactions. Among them, the Fe-Fe interactions are the strongest, and in a first approximation they determine the ordering temperature. Therefore, it is reasonable that when the V concentration is reduced, the number of Fe-Fe interactions is increased and hence the T_C is increased. The non-linearity of the T_C dependence on V concentration is also observed. This non-linearity behaviour has been recently predicted by T. Fukazawa et al.[23] in $RFe_{12-x}Cr_x$ (R = Sm, Nd and Y) at low concentrations of Cr.

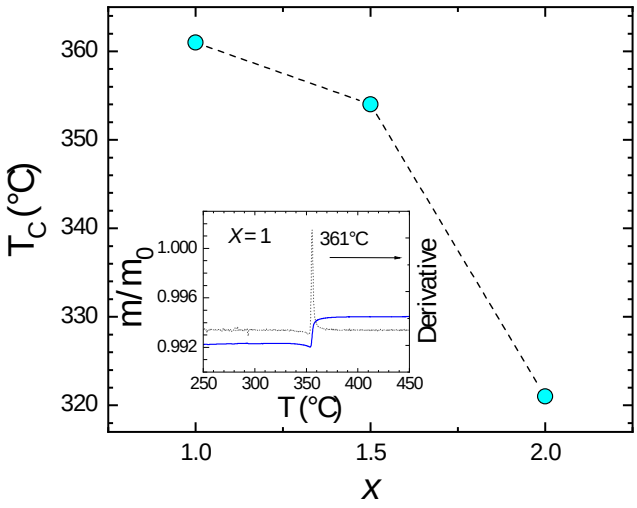

Figure 4: T_C dependence on V concentration x. The inset shows a TGA plot for $x = 1$.

Fig 5. shows the isothermal magnetization curves of oriented powders measured at room temperature along (//) and perpendicular ($\perp$) to the magnetic field. The M_s for $x = 2$ is 83 Am^2/kg (0.81 T, 12.0 μ_B/ f.u.), which is very close to 79.6 Am^2/kg and 85 Am^2/kg reported by Ohashi et al. [11] and Wang et al. [24], respectively. An M_s value of 115 Am^2/kg (1.12 T, 16.8 μ_B/ f.u.) was obtained for $SmFe_{11}V$ ($x = 1$), which is 35% higher than M_s of $SmFe_{10}V_2$ ($x = 2$). Assuming Sm about 1.5μ_B, the magnetic moment per Fe atom would be 1.1 μ_B/Fe ($x = 2$) and 1.4 μ_B/Fe ($x = 1$), which means that magnetic moment per Fe is definitely related with the increase of magnetization when V concentration is reduced. This has a counterpart in the hyperfine field, as it will be discussed below.

The anisotropy field $\mu_0 H_A$ was determined by plotting M in the perpendicular direction as a function of $[(\mu_0 H)^{-2}]$, here a change in the slope of the magnetization at the anisotropy field is expected, because in this point a transition from macroscopic to microscopic spin rotations takes place [25]. The $\mu_0 H_A$ corresponds to the minimum of the $\frac{dM}{d[(\mu_0 H)^{-2}]}$ curve shown in Fig. 5 (b). From these results, it can be seen that $\mu_0 H_A$ for $x = 1$ is slightly higher than $x = 2$, that difference can be attributed to a higher contribution from the second order anisotropy constant K_2 for $x = 1$. An anisotropy field of 9.8 T was obtained for $x = 2$, this value is 1 T higher than the value reported by Grössinger et al. [26], which was determined by means of the singular point detection method using pulsed fields. An effective anisotropy constant was determined by using the equation $\mu_0 H_A = 2(K_1 + 2K_2)/\mu_0 M_s$ [27], and the MAE was determined by calculating the area between the // and $\perp$ direction curves. These results are summarized in Table 1.

x	$\mu_0 M_s$ (T)	M_s (μ_B/f.u.)	$\mu_0 H_A$ (T)	$K_1 + 2K_2$ (MJ/m^3)	MAE (MJ/m^3)	T_C (°C)
2	0.81	12.0	9.8	3.2	1.58	321
1	1.12	16.8	11.0	4.9	1.92	361

Table 1: Experimental magnetic properties of $SmFe_{11}V$ and $SmFe_{10}V_2$.

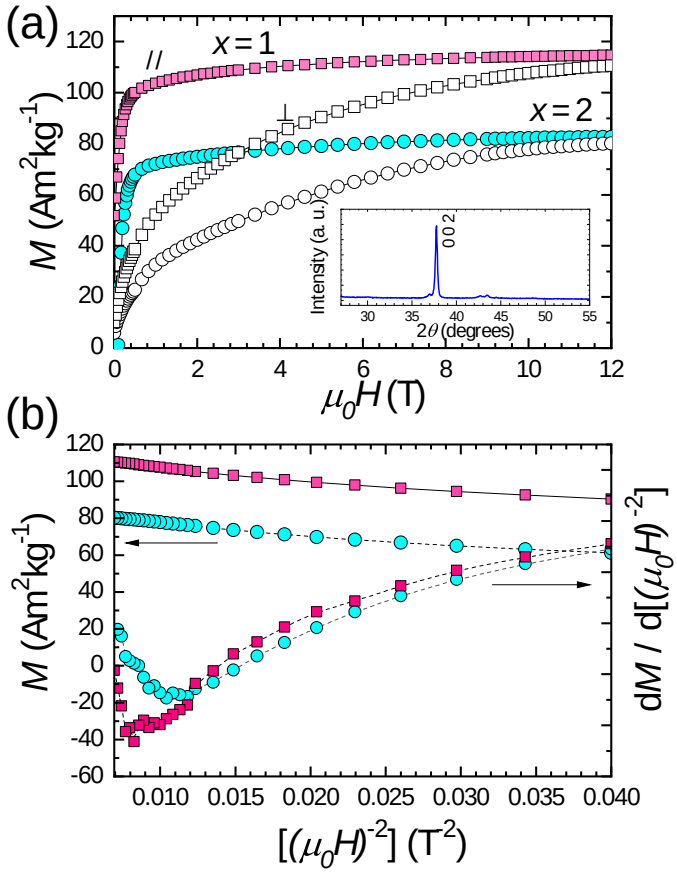

Figure 5: (a) Magnetization curves of magnetically aligned powder particles of $SmFe_{10}V_2$ ($x = 2$) and $SmFe_{11}V$ ($x = 1$) measured at room temperature in parallel (//) and perpendicular ($\perp$) direction to the magnetic field. The inset shows the XRD pattern of the oriented $SmFe_{11}V$ compound, indicating the easy magnetization direction (002) along the c-axis. (b) M and $dM/d[(\mu_0 H)^{-2}]$ as a function of $[(\mu_0 H)^{-2}]$. The anisotropy field is determined from the derivative minimum.

The Mössbauer spectra at room temperature for $SmFe_{12-x}V_x$ alloys, and the fits are shown in Fig 6. The spectra were fitted according to the local environment of each of the three crystallographic Fe sites, $8i$, $8j$ and $8f$, and considering the $8i$ as the preferred site of V atoms. The choice of the $8i$ site for the V atoms was based on the results of previous neutron diffraction studies in $RFe_{12-x}V_x$ (R = Y, Tb, Er, Nd, Dy, Ho, Er) [28, 29, 30]. A visual inspection of the spectra indicates that is necessary to use more than three sextets to fit the spectra.

The statistical distribution of V atoms over $8i$ site modifies the local environment of each $8i$, $8j$ and $8f$ Fe atom, and thus the spectra of $8i$, $8j$ and $8f$ sites are split in a set of subspectra. Each subspectrum corresponds to one different environment around Mössbauer nuclei. The number and the relative areas of each subspectrum was calculated from a binomial distribution [31]. The environments with probabilities lower than 3% were discarded. Nine sextets (3 for $8i$, 3 for $8j$ and 3 for $8f$) were used to fit the spectrum for $x = 1$, eleven (3 for $8i$, 4 for $8j$ and 4 for $8f$) for x = 1.5 and ten (4 for $8i$, 3 for $8j$ and 3 for $8f$) for $x = 2$. The sum of all the subspectra for a given site is presented in each spectrum of Fig 6. The assignment of the $8i$, $8j$, and $8f$ sites was according with Denissen et al. [32], where the site dependence of hyperfine fields follows the condition $8i > 8j > 8f$. The linewidth and the relative subspectra areas were fixed, and the total area of a given site, i.e. the sum of all the subspectra of such site, was a free parameter.

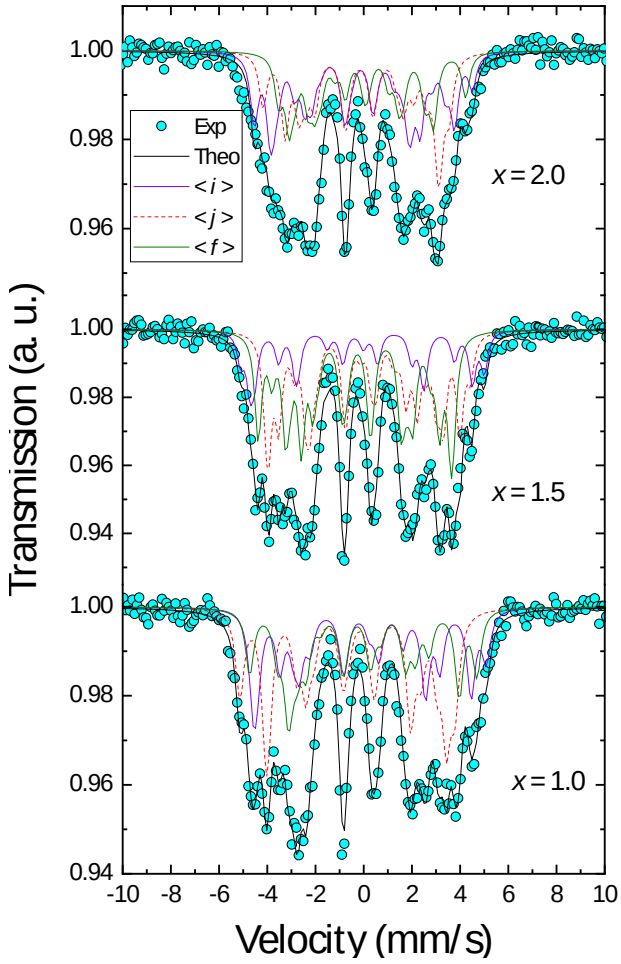

Figure 6: Room temperature Mössbauer spectra for $SmFe_{12-x}V_x$ with different V concentration x.

Average hyperfine fields $\langle B_{hf} \rangle$ and average of isomer shift $\langle \delta \rangle$ of all Fe sites, as a function of V concentration x, are listed in Table 2. As it shows, the contribution of the $8i$ subspectra with the highest B_{hf} values increases when going from $x = 2$ to 1. When the V concentration is reduced, the probability of finding Fe atoms in $8i$ site is higher, then environments with more adjacent Fe atoms are more likely, and the hyperfine fields are larger. This effect can be seen in Fig. 6, when the Mössbauer spectrum of $SmFe_{10}V_2$, appears contracted in comparison with that of $SmFe_{11}V$. A similar behaviour was ob-

x	$\langle\delta\rangle$ (mm/s)	$\langle B_{hf}\rangle$ (T)	$\langle B_{hf}^{8i}\rangle$ (T)	$\langle B_{hf}^{8j}\rangle$ (T)	$\langle B_{hf}^{8f}\rangle$ (T)
2.0	-0.08	21.0	22.5 [1.13]	20.6 [1.03]	19.2 [0.96]
1.5	-0.09	22.0	25.6	21.7	20.3
1.0	-0.15	25.0	26.9 [1.50]	24.6 [1.37]	23.4 [1.30]

Table 2: Mössbauer hyperfine parameters for $SmFe_{12-x}V_x$ (x = 2.0, 1.5, 1.0). Average hyperfine field ($\langle B_{hf}\rangle$), average isomer shift ($\langle\delta\rangle$), and average hyperfine field per site. The values in brackets are assumed moments of Fe in the different sites, in μ_B/Fe.

served by Sinnemann et al. in $GdFe_{12-x}V_x$ and Denissen et al. in $YFe_{12-x}V_x$ series [31, 32]. The increase of B_{hf} values are in agreement with the results of the magnetization measurements, where there is an increase of the average moment per Fe atom from 1.1 μ_B/Fe to 1.4 μ_B/Fe when going from x = 2 to 1.

It is usual that the experimental hyperfine fields are converted to local moments by means of a factor (hyperfine constant), which is considered the same for all Fe sites, and can be defined as the ratio of the average hyperfine field to the average moment per Fe atom. For $SmFe_{11}V$, using μ = 1.4 μ_B/Fe and $\langle B_{hf}\rangle$ = 25.0 T, leads to a conversion factor of 18.0 T/μ_B and for $SmFe_{10}V_2$ a factor of 20.0 T/μ_B. With these factors, we obtained the magnetic moments of Fe at different sites, as the values listed in square brackets in Table 2.

The negative values of $\langle\delta\rangle$ indicate an increase in s electrons charge density at the Fe nuclei in $SmFe_{12-x}V_x$, compared to pure iron [32]. The $\langle\delta\rangle$ decreases with decreasing V concentration. This behavior could be explained in terms of a redistribution of the 4s electron charge with a slightly higher tendency to be around the Fe atoms than V ones. When the V concentration is reduced, the screening effect of the 4s electrons is reduced as well, producing an increase of the s charge density at the nucleus and hence a decrease of the isomer shift.

3.2. Theoretical calculations

Table 3 summarizes the theoretically obtained values of formation of enthalpies, structural and magnetic properties of $SmFe_{12-x}V_x$ (x = 1 and 2). Negative formation enthalpy indicates that the structure is stable. Calculations show that with decreasing concentration of V from 2 to 1 the $SmFe_{12-x}V_x$ structure maintains its stability. The close numbers of the formation enthalpies with one slightly lower for the $SmFe_{10}V_2$ phase might reflect the preferential stabilization of this phase. However, $SmFe_{11}V$ is nearly as stable as $SmFe_{10}V_2$, which is consistent with our experimental results.

x	ΔH_f (eV/u. cell)	V (Å^3)	c/a	M_s (μ_B/f.u.)	$\mu_0 M_s$ (T)	MAE (MJ/m^3)
2	-0.87	339.6	0.5519	12.4	0.85	1.31
1	-0.73	336.4	0.5520	15.8	1.00	1.66

Table 3: Theoretically obtained enthalpy of formation, cell volume, c/a ratio, magnetization and MAE of $SmFe_{11}V$ and $SmFe_{10}V_2$.

As one can see from Table 3, the volume of the structure slightly reduces, but the c/a ratio remains almost unchanged with the decrease of the V concentration. That is in line with the observation made in experiment. The MAE was calculated as the energy difference between the [110] and [001] crystallographic directions. The MAE and magnetic moment of $SmFe_{11}V$ are substantially higher than those of $SmFe_{10}V_2$. Theoretically obtained MAE shows the expected trend, which was also observed in experiment. A 26% increase of MAE was obtained when the concentration of V was reduced from 2 to 1 atom per formula unit. Theoretical values of 1.66 and 1.31 MJ/m^3 for $SmFe_{11}V$ and $SmFe_{10}V_2$, respectively, are in good agreement with corresponding experimental values of 1.92 and 1.58 MJ/m^3 (see section 3.1). We observe also an increase of the magnetization by about 18%; magnetic moment increases due to reduction of V content, which has the spin moment aligned antiferromagnetically to the one on Fe. From the structure, the volume decreases with decreasing V concentration.

4. Conclusions

The intrinsic magnetic properties of $SmFe_{12-x}V_x$ are reported here, both from experimental and theoretical investigations. Hyperfine field, anisotropy field, saturation magnetization and Curie temperature were enhanced as the V concentration was reduced. Theoretically obtained structural and magnetic properties are in good agreement with experimentally obtained values. Our experimental findings and theoretical studies suggest that the $SmFe_{11}V$ compound can be stabilized into the $ThMn_{12}$-type structure. The increased values of saturation magnetization of 1.12 T, the large anisotropy field of 12 T, and the moderate Curie temperature around 361°C make $SmFe_{11}V$ an interesting candidate for permanent magnets applications.

Acknowledgements

This work was supported by the EU Horizon 2020 Programme (grants 686056 and 691235) and the U.S. Department of Energy (DOE DE-FG02-90ER45413). Authors thank to Dr. Iñaki Orue and Dr. Anselmo Tavares for their assistance in high field and Mössbauer measurements, also Dr. Richard Aguirre and Dr. Aleksander Gabay for discussions. The theoretical computations were performed on resources provided by the Swedish National Infrastructure for Computing (SNIC) at PDC and NSC centers. O. E. acknowledges support from STandUP, eSSENCE, the Swedish Research Council and the Knut and Alice Wallenberg foundation (KAW) and the foundation for strategic research (SSF).

References

[1] I. S. Tereshina, N. V. Kostyuchenko, E. A. Tereshina-Chitrova, Y. Skourski, M. Doerr, I. A. Pelevin, A. K. Zvezdin, M. Paukov, L. Havela, and H. Drulis, "ThMn12-type phases for magnets with low rare-earth content: Crystal-field analysis of the full magnetization process," *Scientific Reports*, vol. 8, p. 3595, dec 2018.

[2] Y. Hirayama, Y. Takahashi, S. Hirosawa, and K. Hono, "Intrinsic hard magnetic properties of Sm(Fe1-xCox)12 compound with the ThMn12 structure," *Scripta Materialia*, vol. 138, pp. 62–65, sep 2017.

[3] A. M. Gabay, R. Cabassi, S. Fabbrici, F. Albertini, and G. C. Hadjipanayis, "Structure and permanent magnet properties of Zr1-xRxFe10Si2 alloys with R = Y, La, Ce, Pr and Sm," *Journal of Alloys and Compounds*, vol. 683, pp. 271–275, 2016.

[4] S. Suzuki, T. Kuno, K. Urushibata, K. Kobayashi, N. Sakuma, K. Washio, M. Yano, A. Kato, and A. Manabe, "A new magnet material with ThMn12 structure:," *Journal of Magnetism and Magnetic Materials*, vol. 401, pp. 259–268, mar 2016.

[5] K. Buschow, "Permanent magnet materials based on tetragonal rare earth compounds of the type $RFe12-xMx$," *Journal of Magnetism and Magnetic Materials*, vol. 100, pp. 79–89, nov 1991.

[6] A. Gabay and G. Hadjipanayis, "Recent developments in RFe12-type compounds for permanent magnets," *Scripta Materialia*, vol. 154, pp. 284–288, sep 2018.

[7] R. Madugundo, N. V. R. Rao, A. M. Schönhöbel, D. Salazar, and A. A. El-Gendy, "Recent Developments in Nanostructured Permanent Magnet Materials and Their Processing Methods," in *Magnetic Nanostructured Materials: From Lab to Fab* (A. El-Gendy, J. M. Barandiaran, and R. L. Hadimani, eds.), ch. 6, pp. 157–198, Amsterdam: Elsevier, 1st ed., 2018.

[8] R. Verhoef, F. de Boer, Z. Zhi-dong, and K. Buschow, "Moment reduction in RFe12-xTx compounds (R=Gd, Y and T=Ti, Cr, V, Mo, W)," *Journal of Magnetism and Magnetic Materials*, vol. 75, pp. 319–322, dec 1988.

[9] X. Zhong, F. de Boer, D. de Mooij, and K. Buschow, "Magnetic coupling in the tetragonal rare earth iron compounds of the type R(Fe,V)12," *Journal of the Less Common Metals*, vol. 163, pp. 123–132, oct 1990.

[10] F. De Boer, Y.-K. Huang, D. De Mooij, and K. Buschow, "Magnetic properties of a series of novel ternary intermetallics (RFe10V2)," *Journal of the Less Common Metals*, vol. 135, pp. 199–204, nov 1987.

[11] K. Ohashi, Y. Tawara, R. Osugi, and M. Shimao, "Magnetic properties of Fe-rich rare-earth intermetallic compounds with a ThMn12 structure," *Journal of Applied Physics*, vol. 64, pp. 5714–5716, nov 1988.

[12] J. Yang, S. Dong, Y. Yang, and B. Cheng, "Structural and magnetic properties of RFe10.5V1.5Nx," *Journal of Applied Physics*, vol. 75, pp. 3013–3016, mar 1994.

[13] S. Sugimoto, T. Shimono, H. Nakamura, T. Kagotani, M. Okada, and M. Homma, "Phase Relation of Sm-Fe-V Alloys around the Compound Sm3(Fe,V)29," *Materials Transactions, JIM*, vol. 37, no. 3, pp. 494–498, 1996.

[14] G. Kresse and J. Hafner, "Ab initio molecular dynamics for open-shell transition metals," *Physical Review B*, vol. 48, pp. 13115–13118, nov 1993.

[15] G. Kresse and J. Furthmüller, "Efficiency of ab-initio total energy calculations for metals and semiconductors using a plane-wave basis set," *Computational Materials Science*, vol. 6, pp. 15–50, jul 1996.

[16] G. Kresse and J. Furthmüller, "Efficient iterative schemes for ab initio total-energy calculations using a plane-wave basis set," *Physical Review B*, vol. 54, pp. 11169–11186, oct 1996.

[17] P. E. Blöchl, "Projector augmented-wave method," *Physical Review B*, vol. 50, pp. 17953–17979, dec 1994.

[18] J. P. Perdew, K. Burke, and M. Ernzerhof, "Generalized Gradient Approximation Made Simple," *Physical Review Letters*, vol. 77, pp. 3865–3868, oct 1996.

[19] H. J. Monkhorst and J. D. Pack, "Special points for Brillouin-zone integrations," *Physical Review B*, vol. 13, pp. 5188–5192, jun 1976.

[20] J. M. Wills and B. R. Cooper, "Synthesis of band and model Hamiltonian theory for hybridizing cerium systems," *Physical Review B*, vol. 36, pp. 3809–3823, sep 1987.

[21] J. M. Wills, O. Eriksson, P. Andersson, A. Delin, O. Grechnyev, and M. Alouani, *Full-Potential Electronic Structure Method*, vol. 167 of *Springer Series in Solid-State Sciences*. Berlin, Heidelberg: Springer Berlin Heidelberg, 2010.

[22] P. E. Blöchl, O. Jepsen, and O. K. Andersen, "Improved tetrahedron method for Brillouin-zone integrations," *Physical Review B*, vol. 49, pp. 16223–16233, jun 1994.

[23] T. Fukazawa, H. Akai, Y. Harashima, and T. Miyake, "First-principles Study of Intersite Magnetic Couplings and Curie Temperature in $RFe12-xCrx$ (R = Y, Nd, Sm)," *Journal of the Physical Society of Japan*, vol. 87, p. 044706, apr 2018.

[24] Y. Z. Wang and G. C. Hadjipanayis, "Effect of nitrogen on the structural and magnetic properties of intermetallic compounds with the ThMn12 structure," *Journal of Applied Physics*, vol. 70, pp. 6009–6011, nov 1991.

[25] K. D. Durst and H. Kronmüller, "Determination of intrinsic magnetic material parameters of Nd2Fe14B from magnetic measurements of sintered Nd15Fe77B8 magnets," *Journal of Magnetism and Magnetic Materials*, vol. 59, pp. 86–94, may 1986.

[26] R. Grössinger, R. Krewenka, and K. H. J. Buschow, "Note on the anisotropy fields in tetragonal RFe10V2 compounds," *Journal of Alloys and Compounds*, vol. 186, no. 2, pp. 11–15, 1992.

[27] K. Buschow, "Chapter 4 Magnetism and processing of permanent magnet materials," in *Elsevier Science*, vol. 10, pp. 463–593, 1997.

[28] R. Helmholdt, J. Vleggaar, and K. Buschow, "Note on the crystallographic and magnetic structure of YFe10V2," *Journal of the Less Common Metals*, vol. 138, pp. L11–L14, mar 1988.

[29] R. Helmholdt, J. Vleggaar, and K. Buschow, "Crystallographic and magnetic structure of TbFe10V2 and ErFe10V2," *Journal of the Less Common Metals*, vol. 144, pp. 209–214, dec 1988.

[30] W. Haije, J. Spijkerman, F. De Boer, K. Barker, and K. Buschow, "Magnetic structure of rare earth compounds of the type RFe10V2," *Journal of the Less Common Metals*, vol. 162, pp. 285–295, sep 1990.

[31] T. Sinnemann, K. Erdmann, M. Rosenberg, and K. H. J. Buschow, "A Mössbauer and NMR spectroscopy study of $RFe12-xMx$ intermetallics," *Hyperfine Interactions*, vol. 50, pp. 675–683, jun 1989.

[32] C. Denissen, R. Coehoorn, and K. Buschow, "57Fe Mössbauer study of RFe12-xTx compounds (T = V, Cr, Mo)," *Journal of Magnetism and Magnetic Materials*, vol. 87, pp. 51–56, jun 1990.